Design and Simulation of a Permanent Magnet Electromagnetic Aircraft Launch System

D Patterson, A Monti, C Brice, R Dougal, R Pettus,
D Srinivas, K Dilipchandra
Department of Electrical Engineering
University of South Carolina, Swearingen Center
Columbia, SC 29208 USA
E-mail - patterson@ieee.org

T Bertoncelli
Dipartimento di Elettrotecnica – Politecnico di Milano
Piazza Leonardo Da Vinci, 32 – 20133 Milano – Italy
E-mail: tiziana.bertoncelli@etec.polimi.it

Abstract— This paper describes the basic design, refinement and verification using finite element analysis (FEA), and operational simulation using the Virtual Test Bed (VTB), of a linear machine for an electromagnetic aircraft launching system (EMALS) for the aircraft carrier of the future. Choices of basic machine format and procedures for determining basic dimensions are presented. A detailed design for a permanent magnet version is discussed, and wound field coil and induction machine versions are introduced. The long armature – short field geometry is justified, and in particular the impact of this geometry on the scale of the power electronic drive system is examined.

I. INTRODUCTION

A. The Project

Modern ship designs are increasingly moving towards the use of electricity to distribute, control, and deliver energy for the multiplicity of on-board needs. This trend has already resulted in large direct-drive electric machines for traction in commercial shipping. In some significant cases, including traction, adoption in military applications is rather slower, because of the comparatively low achievable power, energy and torque per unit volume and per unit mass, of electro-mechanical energy conversion systems.

However the benefits of controllability, robustness, reliability, damage management, operational availability, reduced manning, etc., are undeniable. While all actuation systems are under continuous investigation, there is a high level of interest in determining the feasibility of an electromagnetic aircraft launch system (EMALS) for aircraft carriers.

Studies are being carried out at the University of South Carolina (USC) to evaluate alternative design concepts and to determine their feasibility and comparative strengths. Simulation uses the Virtual Test Bed (VTB), a new environment for simulation and virtual prototyping of power electronic systems that includes not only simulation of system dynamics, but also solid modeling of the system and visualization of the system dynamics [1].

EMALS also represents a challenging test case for VTB itself. Models of the different parts of the systems are being built up from the specifications and the characteristics of a typical system, and from engineering design principles.

This work was supported by the US Office of Naval Research (ONR) under grants N00014-1-0131 and N00014-02-0623.

B. The Challenge

The design of an EMALS has many intriguing challenges. The likely specifications and technical features include:

- *Maximum velocity:*- 100 m/s
- *Maximum power stroke:*- 100 m
- *Min braking distance - moving member:*- 10 m
- *Maximum Energy:*- 120 MJ
- *Maximum Thrust:*- 1.3 MN
- *Minimum time between launchings:*- ~50 s.

A typical launch might be for a 25 tonne aircraft accelerated to 75 m/s in 2.7 s, at an acceleration of 2.8 g. This represents a total energy of 70 MJ. Acceleration to the maximum velocity requires a more-challenging 2 s stroke, at a constant acceleration of 5 g.

Whilst the overall system design must include storage, power electronics, and control system design, this paper will concentrate on the electric machine design, and introduce some of the power electronics and control issues.

II. LINEAR MACHINE DESIGN

A. Background

A substantial body of research exists on large linear motors; however, the majority of these are induction machines, and by far the largest number of these are what are known as short primary - long secondary machines. We will also use the terminology short armature - long field for this geometry, a little more apt for non induction machines. Significant issues in design of these machines are the study of both edge effects and end effects [2] [3] [4] [5] [6] [7].

A very common application of short primary - long secondary machines is for traction in electric trains, where the energy is delivered to the train via a catenary or third-rail system, and applied to an on-board armature or primary. The secondary, or field, member is some form of complete track-length reaction rail. The Westinghouse "Electropult", developed during World War II, is an aircraft-launching linear induction machine of this form [8].

This project examines an extensive range of possible electrical machines, permanent magnet (PM) machines, machines with wound field (WF) coil structures (which may

or may not be superconducting), and induction machines, (IM).

The issue of the transfer of >120 MJ in 2 seconds to a moving member (referred to hereinafter as the shuttle) either through sliding contacts or some form of moving harness, is daunting. The "Electropult" referred to above used sliding contacts; however, the thrust required for this EMALS project is about 20 times greater than that delivered by the Electropult. An historical description of the Electropult says, "…the operational costs were so high that in spite of the encouraging performance, steam catapults held the field" [9]. The simplicity of the dc motor driven flywheel and the linear induction machine with a flat "squirrel cage" stator lead one to the conclusion that the operational costs must have been particularly associated with the sliding contacts.The need to decelerate the shuttle also makes minimization of shuttle mass a strong design constraint. These factors, together with the limited length of travel, have led to the initial study of long primary - short secondary, or long armature - short field machines.

B. Basic Machine Sizing

Initial sizing of any machine is often done by considering "Electromagnetic Shear Stress", as defined in Fig. 1.

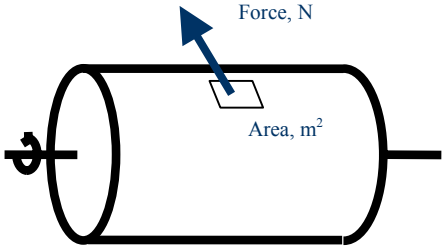

Fig. 1. Electromagnetic Shear Stress Definition.

Miller quotes numbers for typical machines as being between 0.7 and 2 kN/m^2 for fractional horsepower induction machines ranging up to between 70 and 100 kN/m^2 for very large liquid cooled machines such as turbine generators, adding that peak rating may exceed these values by a factor of 2 to 3 [10].

The Electropult, which can be considered as an induction machine with variable resistance "rotor", operated at a stress of a little greater than 50 kN/m^2. This is reasonable for a machine which was highly inefficient, being driven with a constant 60 Hz, and thus spending most of its operational time at a slip of greater than 50%.

It is worth noting that at 100 kN/m^2, for the aircraft launch system to produce 1.3 MN, the active area of the shuttle would need to be in the order of ~13 m^2, or 6.5 m^2 per side in a double-sided structure. Early calculations were based on a structure of roughly this size.

C. Shuttle Mass

It turns out that the issue of stopping the moving member electrically in the minimum distance specified is a particularly

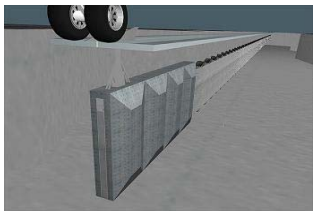

Fig. 2. Inverted U shuttle

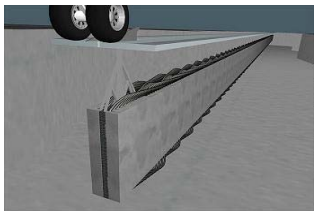

Fig. 3. Blade shuttle

significant constraint on the design. The maximum possible mass that can be decelerated from 100 m/s in 10 metres by applying the reversed electrical thrust of – 1.3 MN, assuming that the acceleration section is well designed at close to achievable limits, is 2.6 tonnes. This mass has a kinetic energy at 100 m/s of 13 MJ, one tenth of the maximum launching energy. Clearly we would want to recover this if possible, and the issue of a friction or water brake (as is used in the steam catapult) to manage 13 MJ regularly is not simple, although a passive "one time use" emergency system must be in place if the normal braking method is electrical active.

The permanent magnet design presented below has a shuttle mass of 2.2 tonnes maximum, and operates at 220 kN/m^2. The wound field machine is designed at 440 kN/m^2, with a shuttle mass of under 2 tonnes.

Alongside electromagnetic shear stress, and indeed integrated into those numbers, current ratings in conductors are often explicitly discussed. Under intermittent loading, maximum workable current densities are between 30 and 50 A / mm^2.

D. Basic Machine Format

In order to achieve the surface area determined by achievable stress figures, two geometries were considered, the "inverted U" and the "blade", as shown in Figs 2 and 3.

While for the inverted U the overall machine will be lighter, the mass of the shuttle must include material for completing the magnetic circuit. The amount of material is strongly dependent on the pole pitch; however, at reasonable values of pole pitch the mass of an iron return path, as required for an induction version, is high, computing to ~ 1 tonne. To this must be added the support structure, and the permanent magnets in the case of a PM machine. For the induction version it will be seen that the weight of the conducting sheet or conducting bars must be realistically ~ 1 tonne, even if the high electromagnetic shear stress levels can be achieved. An option not yet considered in detail would be the use of permanent magnet Halbach arrays on each side [11]. However preliminary calculations still indicate that the 2.6 tonne limit will be difficult to achieve.

In contrast, the blade structure allows the lightest possible shuttle, and a total mass of the two-sided stator, which is within the design goal mass, and also has very good thermal paths.

Of course in practical implementation, the structure will use at least 2 separate blades or inverted U's to allow for the mechanical support structure and the requisite bearings, for much the same reasons as the steam catapult uses two

cylinders and two pistons. However a single blade structure is discussed in this paper, on the understanding that at least in electrical and magnetic terms, multi bladed systems are simply a mechanical transformation of, and can be derived from, the single bladed system.

1) Pole Pitch

Pole pitch is a very significant determinant of machine performance. Short pole pitches usually lead to higher efficiencies (less end turn length), thinner back iron on the stator sections (important for total mass), and are usual in high torque / force machines of large size. Limitations on indefinite reduction of the pole pitch have to do with the fundamental frequency of the drive power, which is also the frequency of flux reversal in parts of the magnetic structure, resulting in core loss, and fringing effects between adjacent poles. These fringing effects are related to the minimum achievable air gap. A pole pitch of 150 mm is currently under consideration, which results in a maximum frequency of 333 Hz in the magnetic circuit of the synchronous versions of the machine.

2) Stator, Slot Dimensions

It has been shown that, at least for surface PM machines, eddy current loss in the stator teeth is proportional to the number of slots per pole per phase [12]. At the minimum one slot per pole per phase, with a traditional overlapping winding, a stator as shown in Fig. 4 has been dimensioned for initial FEA study.

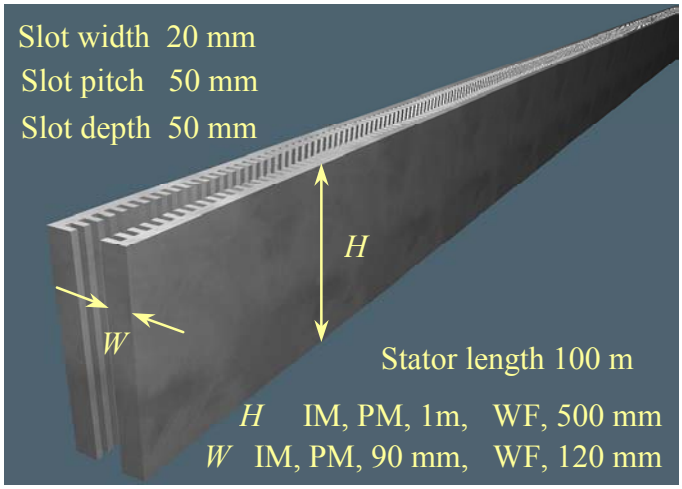

Figure 4. Stator Dimensions

The steel of the PM and induction stator has a total mass of 100 tonnes, and for the wound field coil version 75 tonnes. The maximum allowable total system mass in the design specification is 530 tonnes, and the goal mass is 270 tonnes, so these structures are comfortably inside these specifications.

The thermal mass of the 100 tonne structure is such that an energy dump of 6 MJ, which results for the worst load case in the PM design presented here, will result in < 0.2 degree Celsius temperature rise per shot. Thus active cooling will not be necessary in any part of the PM machine.

As will be seen below, the inductance of the winding is a primary determinant of the complexity of the power electronic drive system, so that the stator is designed with open slots to minimize winding inductance. The stator winding scheme, using the traditional three phases, which are not obligatory but give a good starting position for a first design, is as summarized in Fig. 5.

E. Driving the Armature

Using the permanent magnet machine stress of 220 kN/m^2 as discussed above yields a shuttle length of 3 meters. We begin by assuming standard 6-step servo drive, a pole pitch of 150 mm, a likely achievable flux density in the air gap of 0.9 T, and a total thrust of 1.3 MN. A slot current of 18 kA results.

If this is in a single conductor in the slot, of size 15 * 40 mm (60% fill factor), a current density of 30 A/mm^2 results, yielding an estimated total copper loss of 2 MW for the complete launcher. Since the machine rating is 61 MW the efficiency, considering copper loss only, is thus over 96%.

The more important issue is that, confirmed by FEA, the inductance of the single conductor in the slot is ~ 2.6 μH/meter. Of course the single conductor can be divided, reducing the individual conductor current and the switch current, using more than 1 turn for the winding, without affecting the copper loss (providing the same fill factor results). However the inductance of course goes up as N^2, where N is the number of turns.

Even at 1 turn, the inductance of a single phase 200 metres in length for both sides, pole pitch 150 mm, without considering end turns (where the inductance is much lower, not being in iron), computes to 3.5 mH. In order to commutate from +18 kA to –18 kA at a 333 Hz rate, a supply voltage of 250 kV would be required. Clearly, driving the track in sections is the only feasible option.

F. Simulation

Discussion so far has indicated the very large range of possibilities that need to be compared and considered when conceiving of a system of this complexity. Most commonly, promising research directions are deduced from data taken from existing operating systems. Without operational systems to guide research, recourse must be had to very powerful cross-disciplinary system simulators.

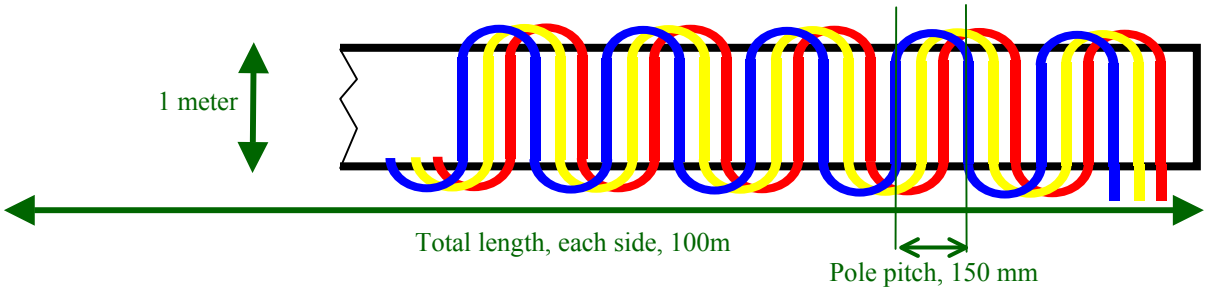

Fig. 5. 3 phase, 1 slot per pole per phase, stator winding (armature) structure.

1) VTB

VTB is an ideal tool to explore the many possible variants for an EMALS, and to facilitate convergence on optimal solutions. The project is enabling experience in machine design and simulation to be applied to a very detailed study of this very large pulsed power application, focusing on a range of important criteria. These include total system mass, total system volume, thermal management, reliability, robustness, survivability via redundancy, and also acoustic, magnetic, and electromagnetic signatures. These considerations are in addition to very real challenges in the many control loops in an EMALS, up to and including totally sensorless control.

III. Detailed Machine Design

In this research project, the majority of effort has so far been directed to the permanent magnet version of this machine, which has resulted in a surprisingly simple and achievable design. Some effort has been expended to explore the wound field coil, which has some intriguing implications, and less effort on the induction version, since this is an area where a substantial body of expertise exists. Each of the three types is considered separately below.

IV. Permanent Magnet Machine

At the pole pitch of 150 mm discussed above, a 3 meter shuttle would involve some 20 blocks of Neodymium Iron Boron (Nd Fe B) magnet material, supported in a composite structure. The magnet thickness is determined by two things,

(a) the minimum feasible airgap and the design requirement for near to 0.9T in that airgap, and

(b) the requirement that the slot current of 18 kA not demagnetize the permanent magnet material.

The design analyzed uses an 8 mm airgap on each side, and a total magnet thickness of 80 mm. Using 120° magnet widths, the total magnet mass for the shuttle computes to 1184 kg. At 100 m/s, and increasing the mass by 40% for the supporting composite structure, the shuttle has a kinetic energy of 8.3 MJ. Using the same winding scheme as for launching, producing a reverse thrust of 1.3 MN, this shuttle can be stopped electrically, with full energy recovery, in 6.4 meters, well inside the allowed distance of 10 metres. The stopping time is 127 ms, and the deceleration is ~ 80g, so the support structure must be designed to manage this deceleration for the material, as well as the transference of the thrust to the airframe during acceleration.

A. Finite Element Analysis

2D FEA has been used to verify certain aspects of the design, and to make refinements.

1) Demagnetization

The shuttle with 120° (100 mm) magnet widths, and 20 poles of alternating polarity, begins and ends with a half-width magnet. For simplicity in modeling, the analyzed shuttle had a length of 5 pole pitches. The shuttle begins and ends with a half-width pole, for a total of 6 magnetic poles, as shown in fig. 6. Note that only half of the geometry is entered, invoking

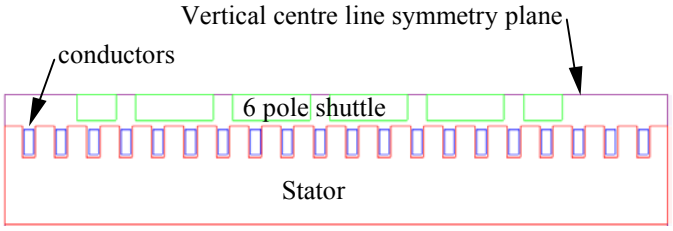

Figure 6. Geometry used for FEA

symmetry around a center line. Thus the drawing is of a top view of one side of a short section of the complete machine.

This model was analyzed for the vertical component of B in the magnets with 18 kA in the conductors, at a range of horizontal positions of the shuttle. At each position the field plot was checked. At no stage is the B in the material reduced below 0.4 T in the direction of magnetization so that demagnetization is not an issue. The magnet thickness used here is necessary only to keep a very high flux density in the chosen air gap. Clearly, other designs could use a higher electric loading and a lower flux density with less magnetic material and less shuttle mass; however, those designs would require higher di/dts in the windings. As we shall see, this impinges seriously on the overall operation.

2) Thrust Linearity

Rectangular magnets and open slots as shown above are capable of developing very substantial cogging forces, which themselves are indicators of variation in permeability, which result in increased iron loss, due to flux ripple. The magnet width can be adjusted to control this cogging force, usually at the cost of increased ripple in the back emf. In this intermittent duty machine iron loss is not a serious issue; however, any thrust ripple adds extra unwanted stress to the airframe. While thrust ripple can be controlled by current control, the option to minimize thrust ripple, without considering cogging force, by adjustment of magnet width, was exercised with surprisingly effective results.

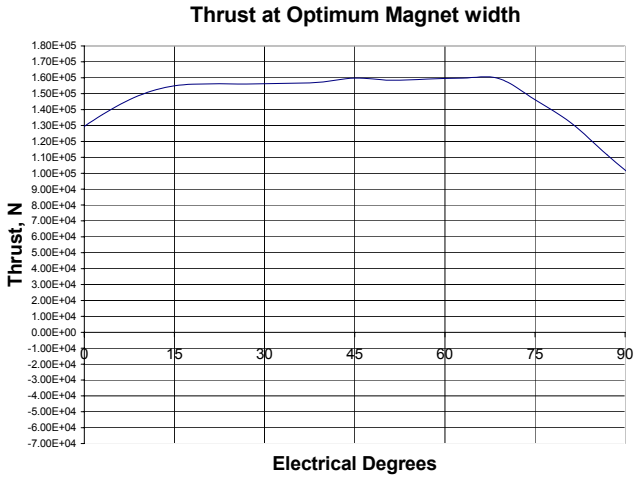

Fig. 7. Thrust determined by FEA for constant current in two phases, as a function of shuttle position in electrical degrees

Fig. 7 shows the thrust as a function of position with two windings energized with constant current, as is usual with simple 6-step switching. Since each phase will be independently controlled, handover at the edges of the each step can be managed to provide a smooth transition from one phase pair to the next. This shuttle would have a slightly higher mass than that discussed above; however, such a small increase is quite manageable.

B. Power Electronics

While the machine design turns out to be surprisingly simple, the power electronics design, particularly with the long armature – short field geometry, is challenging, and very much dependent on the ratings of available switches. As discussed above in section II.*E*, the track must be sectioned into driveable lengths. In order to provide a high level of control, to provide high levels of redundancy, and to provide the option to use other than three phases, it was decided to drive each separate phase winding in each section independently, with its own H bridge.

1) Typical Devices

A very promising device, and one for which USC has been developing models, is the IGCT. One of the principal models developed is for a device with a rating of 4 kV and 2.4 kA. Two of these in parallel can be used as a switch element to make an H bridge with 4 kV 4.8 kA ratings. This configuration has been adopted for the early simulations. In order to manage 18 kA in each slot, it was decided to use 4 independent turns in each phase, each with its own H bridge, so that in any section of the track. 3*4=12 H bridges are required.

2) Sectioning the Track

At every point along the 100 meter track a maximum driveable inductance can be calculated, based on the maximum possible velocity at that point. For example, at the end of the track the maximum velocity is 100 m/s. The ΔI is from - to + 4.8 kA, or 9 kA, the ΔT is, from the velocity and the pole pitch = 0.5 ms, the E manageable by the bridge is 4 kV, resulting a in an $L_{max,\ 100\ meters}$ of 0.22 mH.

This inductance results from both sides of 5 meters of track for a single turn of a single phase. This winding starts at 100 meters on say the left hand side of the track, goes back to 95 meters, crosses underneath and then returns from the 95 meter point to the end at 100 meters. Thus the final section of the track to be driven, given the available switches, can be only 5 meters in length.

An expression for the driveable length at any point in the track ΔX can be derived as

$$\Delta X = \frac{V_b p_p^2}{6 L_s D_s \Delta I \sqrt{2ax}} \qquad \text{,.....(1)}$$

where V_b is the available bus voltage, p_p is the pole pitch, L_s is the inductance/meter in the slot, D_s is the depth of the slot, ΔI is the current change, a is the acceleration and x is the distance along the track. This formula has been derived for 6-step switching, commutating the current by ΔI in 1/6 of a period. The back emf does not appear on the assumption that for a trapezoidal back emf, the average back emf over this time interval is zero.

Note particularly the significance of pole pitch, so that track sectioning can be dramatically reduced by increasing the pole pitch.

The equation above is for a fixed physical design, and is of the form

$$\Delta X_n = kx^{-1/2}$$

which for the machine constants of this design, is graphed in Fig. 8. Applying this sectioning to the design results in 12 sections, increasing in length from 5 to 15 meters for the initial section

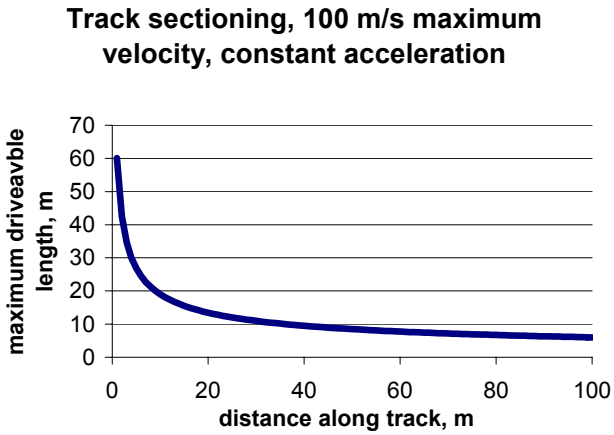

Figure 8, Track section length as a function of position

No more than two sections are ever activated at any one time, since the shuttle of 3 meter length is shorter than any section. Therefore, in operation, section 1 of the track is activated, and the shuttle begins to move. As the leading edge of the shuttle arrives at the start of section 2, section 2 is activated as well, and then as the trailing edge of the shuttle leaves section 1, section 1 is deactivated. The H bridge set that was driving section 1 can be disconnected from section 1, and connected to section 3 in readiness for the arrival of the leading edge of the shuttle at the start of section 3.

3) Power Electronics Switching Matrix

Thus a workable switching matrix involves 2 sets of 12 H bridges. Connection of each bridge in a set to one of 6 sections (one set drives sections number 1,3,5,7,9, and 11, the other set drives the even numbers) can be done using back-to-back thyristors. These thyristors would be continuously triggered when required, and will switch off when the current decays to zero, when the H bridge switches are no longer driven. There is adequate time in all cases for this to happen. Figs. 9 and 10 show the overall matrix structure, and the H bridge – thyristor connections, respectively.

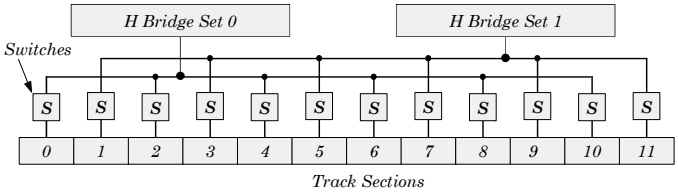

Fig. 9. Overall Switching Matrix

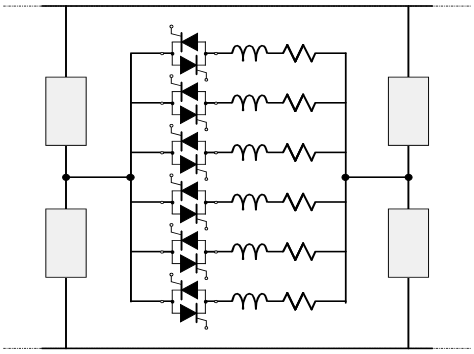

Fig. 10. The H - Bridge – Thyristor - Winding connections

V. VTB Simulation

The authors are currently refining models for all of the individual system components. The current status of the simulation is reported below. A simulation-driven animation of the 3D system showing the obtainable performance has been produced. Effort is currently being concentrated on the permanent magnet brushless motor case.

A. Machine modeling

A standard d-q model has been developed for a generic PM machine [13]. This has been adapted, replicating in the modeling structure the modularity of the EMALS motor. The model architecture has two separate parts, the stator winding models (one for each section), and the shuttle model. The system is designed so that any set of independent stator section models can be connected to a single shuttle.

The stator model simulates the current in each single winding in a section, and it defines the force contribution of that section to the overall system force. The superposition theorem is applied in the shuttle model to sum the force generated by each winding in each section and then to solve the mechanical equations for speed and position. This information is sent back to the stator sections in order to evaluate the back electromotive force.

The equivalent circuit of each stator section model is shown in Fig. 11. Each winding is represented by its equivalent circuit. Since the design suggests 4 turns for each phase, the model has the 12 independent circuits for the three phases in any single section.

The evaluation of the electromotive force and the mechanical force coefficient is based on the mechanical position and velocity. First of all a check is performed to evaluate if the shuttle is over the section, so that the action of the permanent magnet is present, and then a check of the position within the section determines the specific values.

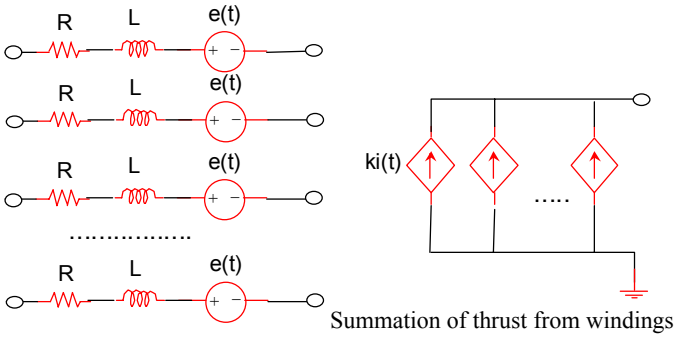

Fig. 11: The equivalent circuit of the stator model

In particular for the evaluation of the thrust, the following equation is adopted:

$$T = K_p n \sum_{k,j} \left(\frac{\partial \psi}{\partial x} \right)_{k,j} i_{k,j}$$

where:

- $i_{k,j}$ is the current in the j-th winding of the k-th phase
- $\left(\frac{\partial \psi}{\partial x} \right)_{k,j}$ is the derivative of the flux of the permanent magnet with respect to distance, as seen by the j-th winding of the k-th phase
- n is the number of pole pairs
- K_p is a coefficient introduced to manage the amount of overlap of the shuttle and stator section p. If the shuttle is completely over a section p this coefficient will be unity. This is illustrated in Fig. 12 for p = 2.

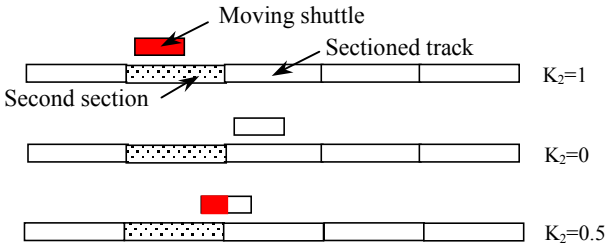

Fig. 12. Definition of coefficient K_2, (for the second section)

The shuttle is modeled through the equivalent circuit shown in Fig. 13.

This circuit has two separate sections. The velocity is calculated by summing the forces from all the 12 sections, subtracting the losses, and having this resultant thrust acting on the mass of the shuttle represented by a capacitor to provide the integration. The position calculation is then obtained as an integration of the velocity.

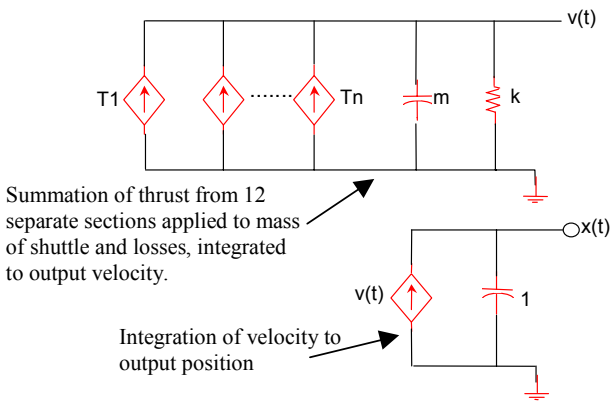

Fig. 13: The equivalent circuit of the moving part

A set of tests was performed to validate the modeling approach. The VTB schematic for first test is in fig. 14.

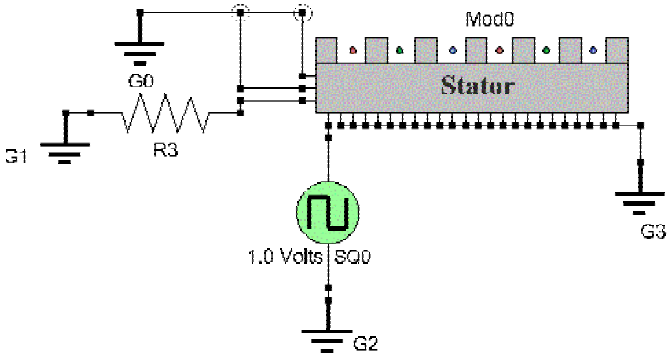

Fig. 14. VTB schematic for first simulation test

The pins on the bottom are the electrical terminals, while those on the left are for the mechanical interface. In this case the speed and position are fixed to zero (the two pins on top are grounded – equivalent to a locked-rotor test), while a square wave voltage feeds one winding. This test verifies the correctness of the electrical subsystem and a classical R-L transient is the computed result as seen in Fig. 15.

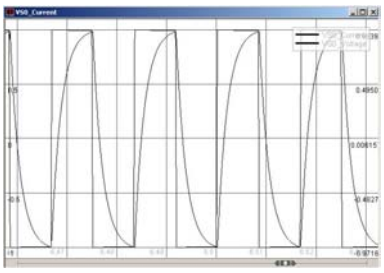

Figure 15. The results of the first test

A second test, with the VTB schematic as in Figure 16, validated the mechanical model. In this case we have three stator section models and one shuttle model. A constant velocity is applied to the shuttle and then we measure the voltage across the open-circuited stator electrical windings.

In this case we see in Figure 17 the classical trapezoidal waveform that appears only for those sections that are under the shuttle. We also see the amplitude being related to overlap,

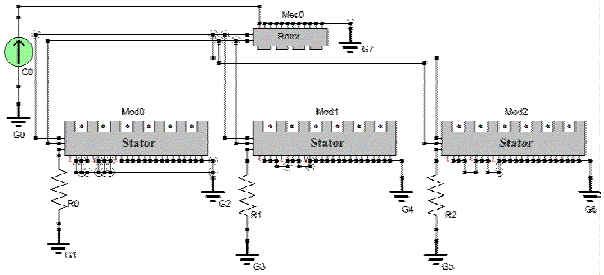

Fig. 16. VTB schematic for second simulation test

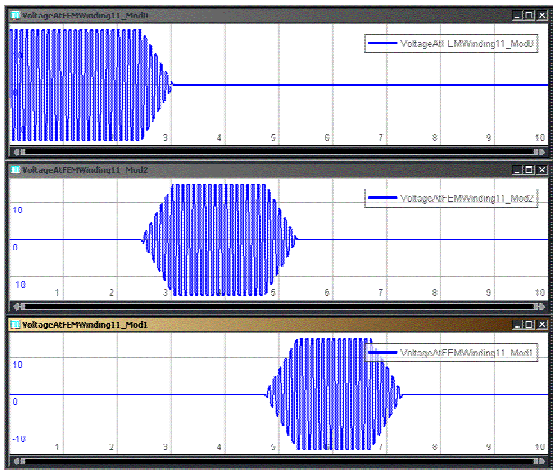

Fig. 17 Back emf in the first three sections of the track, shuttle moving with constant velocity

via the factor *Kp*, and we see that successive sections are of different length.

B. Converter modeling

All the switching alternatives are considered. A completely separate drive circuit for each coil is seen as the best solution, although the issue of current control of the magnetically coupled coils in the same slot has yet to be addressed. Averaged models of PEBB-like converters have been used to speed up the simulation; but switched versions can also be used.

In the first simulation a single H bridge configuration for each phase was adopted: This means that a single converter was connected to 4 different windings in parallel. This is reasonable since we are using ideal switch models at this stage.

C. Control modeling

The controller was modeled by using the VTB-Simulink interface. The controller is designed to fulfill the following requirements:

- each independent coil is fired by shuttle position sensors located along the stator,.
- preset current (thrust) levels in each coil are known,
- open-loop operation is possible if communication fails or is damaged,
- if communication exists, each coil thrust is adjusted as it is firing, so as to ensure adherence to the required thrust/ velocity profile.

The control algorithms are designed in Simulink, tested interactively, and finally compiled for better simulation performance.

The modular structure of the motor requires a hierarchical structure for the thrust control. Only one thrust control (System Manager or SM in the following) is used, and as many current controllers (Hardware Managers or HM in the following) as the number of H bridges. The SM will decide from shuttle position information, in which sections to control current

Fig. 18 shows the structure of the SM. According to the actual shuttle position, the reference for each section is generated by a "section selector" block. Each HM receives a current reference and implements the current strategy as shown in Fig. 19.

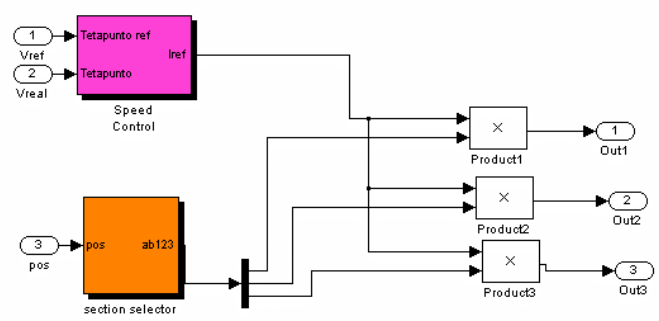

Fig. 18. The SM structure in Simulink

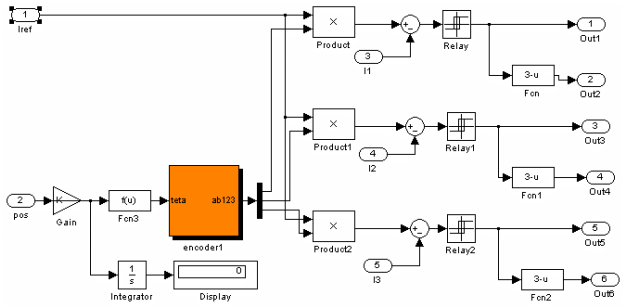

Fig. 19. The HM structure in Simulink

VI. Wound Field Machine

Work to date has involved the FEA modeling of a system with the stator dimensions discussed in section 2.D.2. Initial runs have been carried out using a one-turn field current of 120 kA. This produces ~ 2T in the airgap, so that the back emf per section is exactly as for the PM machine, and the same currents produce ~ twice the shear stress, and therefore the same total thrust. Since the inductance is halved by halving the conductor lengths, the track sectioning is reduced significantly. Further work will optimize the coil design. While it was initially thought that this shuttle would need to be superconducting, it turns out that because of the very short operational time a version using copper coils and carrying ultracapacitors is possible. An early design includes 1200 kg of copper and 400 kg of ultracapacitors to provide the 6.6 MJ required to operate the coils for 5 seconds, the maximum launch time. The temperature rise of the copper in this 5 seconds is ~ 14° C, so that some form of cooling between firings would be necessary. Many options exist to lower the temperature dramatically before each launching, thus reducing the field winding copper losses during launching. Further, optimization of the aspect ratio of the shuttle may make such a non-cryogenic design more feasible.

One of the significant implications of increasing the airgap flux density is that the tooth iron fully saturates, so that the flux density in the slot, and thus in the copper conductors, increases dramatically. This exposure to very high dB/dt s can result in massively increased eddy current losses in the copper conductors. Fig. 20 shows the instantaneous power loss in the four conductors in a single slot when the shuttle passes over them at 100 m/s, as a function of the air gap flux density. Clearly, while lamination will easily control the losses at ~ 1 T with the PM machine, the wound field machine will require much more aggressive attention to conductor stranding.

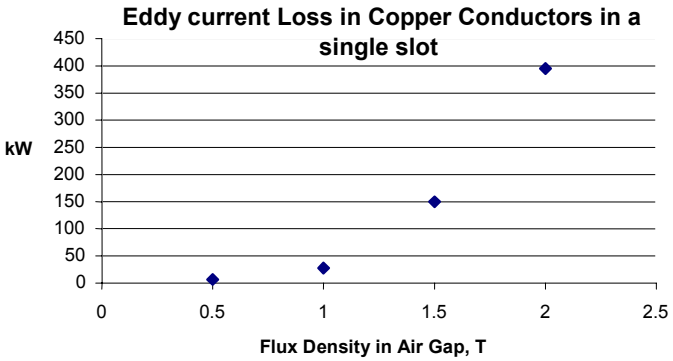

Fig. 20. Instantaneous power loss in the four conductors in a single slot when the shuttle passes over them at 100 m/s, as a function of the air gap flux density.

VII. Induction Machine

After completing analysis of the wound field coil machine, a more traditional induction machine will be designed, analyzed, and simulated. However, what can be said at the outset, is that for the same format as the PM machine, and using the same mass, i.e. ~1200 kg of copper in sheets or coils ideally placed and carrying the current required to provide the same thrust, these coils would have a temperature rise of ~ 8° C per shot. Thus either the shuttle needs to be cryogenic or some form of active cooling will be necessary [14]. Then we must arrange to induce that current with an additional magnetizing current in the stator. This has an immediate impact on the track sectioning, since the ΔI in the track sectioning equation, (1), increases. Any design attempts to increase the flux in the airgap for the same current must increase the inductance by definition, and this again appears in (1). Once any section gets to be shorter than the shuttle itself, the quantum of power electronics switches (for driving e.g. three sections simultaneously) begins to increase dramatically. Thus the induction version will be expected to, for similar layouts, require active cooling and have a larger amount of power electronics. The induction motor system will be substantially more difficult to drive, since the magnetic circuit

would be designed to maximize the flux in the airgap from current in the armature. Thus the inductance of the armature winding will be higher, and the mutual inductance between phase windings will not be negligible. The results of this work will be reported at a later date.

VIII. Conclusions

We conclude that the PM machine is a very good solution, being surprisingly small and simple, with a manageable but large power electronics switching system. The wound field coil machine does not appear to provide sufficient advantage to justify the extra complexity, unless weight becomes a much more significant concern, but this configuration does have advantages in the power electronic system. The induction machine design will be very complex, requiring either cryogenics or active cooling, and the cost of the power electronics is liable to be substantially higher because of the higher inductances.

A more global conclusion is that in relation to large machines, considering PM, IM or WF types, the remarkable benefit of the PM design is twofold.

Firstly it provides the ability to build structures with minimal inductance because of very large effective airgaps, resulting from the permeability of the Nd Fe B being ~ 1.

Secondly a significant thermal penalty is avoided by using a permanent magnet rather than its equivalent model, a one turn loop current. This thermal penalty occurs in ambient temperature wound field machines as well as in induction machines.

IX. Post Script – De-risking the Technology

This work on a large-scale system with no physical demonstration has produced more than the usual number of concerns and doubts about the viability of, as one example, managing the very large forces of attraction. As evidence that these forces can be managed, and that such a large PM linear machine is indeed viable we cite a PM roller coaster launcher which was installed in 2000 at Six Flags in Holland [15]. Fig. 21 shows this system, in which a shuttle launches the roller coaster. The fin in the center below the shuttle provides reaction for the bearings which maintain the ~10 mm airgap either side of the double armature This machine is of the double inverted U layout, one on each side. It operates at a stress, estimated, using some given dimensions to be 80 kN/m^2, and has a thrust ~3 times that of the WWII Electropult. An installation of the same form has been in operation at Disneyworld in Orlando Florida since July 1999, with continuous operation for up to 21 hours per day, a 48 second dispatch time and operating 365 days per year. In the 40 months since the ride has been open to the public it has achieved a total number of launches in the region of 1.2 million. There have been no equipment failures during this time [16].

X. Acknowledgments

This work was supported by the US Office of Naval Research (ONR) under grants N00014-1-0131 and N00014-02-0623.

Fig. 21. Linear PM coaster launcher at Six Flags Holland. (Photograph by kind permission, KumBak Coasters)

XI. References

[1] R. Dougal, T. Lovett, A. Monti, E. Santi "A Multilanguage Environment for Interactive Simulation and Development of Controls for Power Electronics", IEEE Power Electronics Specialists Conference, Vancouver, Canada, June 17-22, 2001.

[2] S. Yamamura, "Theory of linear induction motors", John Wiley and Sons, 1972

[3] I. Boldea, S. A. Nasar, "Linear Motion Electromagnetic Systems", John Wiley and Sons, 1985

[4] I. Boldea, S. A. Nasar, "Linear Electric Motors: Theory, Design and Practical Applications", Prentice-Hall, 1987

[5] S. C. Ahn, J. H. Lee, D. S. Hyun, "Dynamic Characteristic Analysis of LIM Using Coupled FEM and Control Algorithm" IEEE Transactions on Magnetics, vol. 36, No. 4, July 2000, pp. 1876-1880

[6] K. Davey "Pulsed Linear Induction Motors In Maglev Applications" IEEE Transactions on Magnetics, vol. 36, No. 5, September 2000, pp. 3703-3705

[7] J. Faiz, H. Jafari, "Accurate Modeling of Single-Sided Linear Induction Motor Considers End Effect and Equivalent Thickness" IEEE Transactions on Magnetics, vol. 36, No. 5, September 2000, pp. 3785-3790

[8] "A wound Rotor Motor 1400 Feet Long" Westinghouse Engineer, September 1946, P160-161.

[9] http://historia.et.tudelft.nl/pub/art/machines.php3#III3

[10] T J E Miller Brushless, Permanent-Magnet and Reluctance Motor Drives, OUP 1989.

[11] Post R F " The Inductrack Approach to Magnetic Levitation" Record of the 16th International Conference on Magnetically Levitated Systems and Linear Drives, MAGLEV 2000, Rio de Janiero, Brazil, June 2000

[12] Chunting Mi, Gordon R. Slemon and Richard Bonert, "Modeling of Iron Losses of Surface-Mounted Permanent Magnet Synchronous Motors", Record of the 36th Annual IEEE Industry Applications Society Conference, IAS '2001 Chicago, October 2001.

[13] I. Boldea, S. A. Nasar, Linear Electric Actuators and Generators, Cambridge University Press, 1997

[14] R J Elwell, R W Garman, M Doyle " Thermal Management Techniques for an Advanvced Linear Motor in an Electric Aircraft Recovery System" IEEE Transactions on Magnetics,. Vol 37, No 1, January 2001, pp 476 – 479.

[15] D Vatcher, J Uittenbogaart "Linear Synchronous Motor Technology for Launching Roller Coasters" Record of the Trends in Leisure and Entertainment Conference and Exhibition 2000, (TiLE 2000)

[16] D Vatcher, Kum Bak Coasters, personal correspondence